Caspase-7 uses an exosite to promote poly(ADP-ribose) polymerase 1 proteolysis

Dave Boucher, Véronique Blais, and Jean-Bernard Denault

Institut de Pharmacologie de Sherbrooke, Department of Pharmacology, Faculty of Medicine and Health Sciences, Université de Sherbrooke, Sherbrooke QC, J1H 5N4, CANADA

Running title: **Caspase-7's exosite**

Keywords: **caspases, exosite, PARP, p23, apoptosis**

Correspondence should be addressed to J.-B.D.
Université de Sherbrooke
Department of Pharmacology
Faculty of Medicine and Health Sciences
3001, 12th Avenue N.
Sherbrooke QC, J1H 5N4
CANADA
Phone: +1-819-820-6868 ext. 12789
Fax: +1-819-564-5400
Email: Jean-Bernard.Denault@USherbrooke.ca

Abbreviations used: cyt*c*, cytochrome *c*; ICAD, inhibitor of caspase-activated DNAse; NTD, N-terminal domain; PAR, poly(ADP-ribose); PARP-1, PAR polymerase 1; XIAP, X-linked inhibitor of apoptosis protein.

Abstract

During apoptosis, hundreds of proteins are cleaved by caspases, most of them by the executioner caspase-3. However, caspase-7, which shares the same substrate primary sequence preference as caspase-3, is better at cleaving poly(ADP-ribose) polymerase 1 (PARP) and Hsp90 co-chaperone p23, despite a lower intrinsic activity. Here, we identify key lysine residues (K^{38}KKK) within the N-terminal domain (NTD) of caspase-7 as critical elements for the efficient proteolysis of these two substrates. Caspase-7's NTD binds PARP and improves its cleavage by a chimeric caspase-3 by ~30-fold. Cellular expression of caspase-7 lacking the critical lysine residues resulted in less efficient PARP and p23 cleavage compared to cells expressing the wild-type peptidase. We further show using a series of caspase chimeras the positioning of p23 on the enzyme providing us with a mechanistic insight into the binding of the exosite. In summary, we have uncovered a role for the NTD and the N-terminal peptide of caspase-7 in promoting key substrate proteolysis.

\body

Introduction

Apoptosis employs a family of cysteinyl peptidases, the caspases, to integrate and propagate various signals to cause cell demise. The latter step is governed by a subgroup of caspases named executioners that are responsible for the cleavage of a plethora of cellular proteins. The cleavage of some of these proteins provokes the associated hallmarks of apoptosis (1, 2). A survey of the published literature suggests that, among executioners, caspase-3 performs the bulk of the cleavage events. These data are in agreement with biochemical studies suggesting that this caspase is highly active and is present at the highest concentration among all caspases in most cells (3-5). For these reasons, caspase-3 supersedes other caspases in most biochemical readouts (4).

Caspase-3 and -7 share 57% sequence identity throughout their catalytic domains. Additionally, they have the same substrate preference based on studies using peptide substrate libraries (6, 7). Despite this apparent redundancy, they have an overlapping but non-redundant substrate repertoire. For instance, ROCK1, α-fodrin and Rho-GDI are cleaved efficiently by both caspases (8, 9). However, ICAD (9), the XIAP (X-linked inhibitor of apoptosis protein) (10) and initiator caspase-9 (11) are preferred by caspase-3, whereas Nogo-B (12), ataxin-7 (13), and the p23 co-chaperone (9) are cleaved more efficiently by caspase-7. PARP-1 [poly(ADP-ribose) polymerase 1], the first caspase substrate identified (14), is a particularly interesting death substrate, and its cleavage is now recognized as a hallmark of apoptosis. PARP-1 proteolysis is essential for an adequate energetic balance during apoptosis and protects against necrosis (15, 16). Previous work has suggested that caspase-7 is responsible for PARP inactivation during apoptosis (17), but no mechanism for such selectivity has been proposed. However, many caspases and the immune-derived granzymes have been suggested to cleave PARP (14, 17-21). Notably, whereas PARP-1 is cleaved at a canonical caspase-3/7 site (DEVD↓G), p23 is cleaved at a less suitable site (PEVD↓G). Indeed,

studies have shown that a proline instead of an aspartate in the P4 position reduces the catalysis of caspase-7 by 16,500-fold (7).

In the present study, we hypothesized that if caspase-7 is better at cleaving certain death substrates such as PARP and p23 despite the fact that it is intrinsically less active than caspase-3, it must use exosites to improve catalysis. This attractive possibility has been raised several times in the past decade (22-25), but never confirmed. Our results show that the N-terminal domain (NTD) of caspase-7 contains a conserved basic patch that greatly improves substrate recognition and proteolysis of both death substrates. This study provides a unique demonstration of the use of a substrate exosite by a caspase.

Results

Caspase-7 cleaves PARP and p23 more efficiently than caspase-3. To determine whether caspase-7 or caspase-3 is the more efficient protease at cleaving death substrates, we performed assays in which active site-titrated recombinant caspases were incubated with cell extracts from MCF-7 cells (which lack caspase-3) expressing a short hairpin RNA against caspase-7 (Supplementary **Fig. 1***A*). In these conditions, the ectopic caspase faces a mixture of substrates, akin to the cellular context. Furthermore, at the concentration used, caspase-7 cannot activate other caspases (26). When various concentrations of caspase-7 or -3 were incubated with the extracts, the 116 kDa full-length PARP was cleaved by both enzymes to yield the typical 89 kDa fragment detected by our antibody (**Fig. 1***A*). However, whereas 5 nM caspase-7 was sufficient to process > 85% of PARP, 50 nM caspase-3 resulted in less than 40% conversion. We also examined the cleavage of p23 and found that caspase-7 cleaves this protein more efficiently than caspase-3, albeit with less efficacy than PARP (**Fig. 1***B*). To ensure that our assays were unbiased towards caspase-7, we analyzed ICAD and recombinant caspase-9 proteolysis and found that caspase-3 is better at cleaving both proteins (**Fig. 1***C,D*). These results demonstrate that each of these executioner caspases prefers a different set of death substrates.

Comparison of the activity of these enzymes using the small fluorogenic substrate AcDEVD-Afc yielded catalytic specificity constants (k_{cat}/K_M) for caspase-7 and -3 of 1.1 x 10^5 and 5.9 x 10^5 $M^{-1}s^{-1}$, respectively (Supplementary **Table SI**), which are in agreement with previously published work (4, 26, 27). To determine whether the observed difference was an artifact of using a peptidic substrate, we used the baculovirus caspase inhibitor p35 with the inactivating C2A mutation that turns this protein into a substrate (28, 29). Similar to AcDEVD-Afc, p35-C2A is cleaved ~5 times more efficiently by caspase-3 than by caspase-7 (**Fig. 1***E*), suggesting that caspase-3 is indeed a more proficient enzyme. We also tested the activity of caspase-3 and -7 on AcPEVD-Afc, which features the same cleavage site motif as that in p23, and found that caspase-3 is ~500 times more active than caspase-7 (Supplementary **Table SI**). Finally, to ensure that the preference for PARP we observed is not caused by the presence of competing substrates or endogenous caspase inhibitors such as XIAP, we performed assays using antibody-purified PARP (**Fig. 1***F*). However, we still found that caspase-7 was more efficient than caspase-3 at cleaving purified PARP, demonstrating the robustness of our

assays. Taken together, these results suggest that caspase-7 likely uses an exosite to promote PARP and p23 cleavage.

The mature NTD of caspase-7 promotes PARP cleavage. The catalytic domain of caspase-3 and -7 is highly similar. However, the N-terminal region that precedes the catalytic domain is much longer in caspase-7; this region, therefore, is a good exosite candidate. Consequently, we tested the ability of a caspase-7 variant that lacked part of its NTD to cleave PARP. We took advantage of an alternate translation initiation site within the NTD (Met45; **Fig. 2***A*) to generate an active enzyme (26). M45-caspase-7 is less efficient at cleaving PARP than wild-type (WT) enzyme at identical concentrations (**Fig. 2***B*), even though it is as active on the peptidic substrate (Supplementary **Table SI**). The percentage of PARP cleavage was estimated using imaging software as described in Supporting information and reported in Supplementary **Fig. 2**. Specifically, we compared the intensity of the full-length 116-kDa protein because the cleaved fragments have variable detectability and stability as suggested for many caspase substrate cleavage products including PARP (30). By readjusting the caspase concentration and incubation time, we were able to estimate that proteolysis of PARP by caspase-7 is nearly 8 times higher than that by caspase-3, and that the cleavage rate by truncated M45-caspase-7 was less than 2×10^4 $M^{-1}s^{-1}$, which is ~30 times lower than the rate by WT caspase-7 (**Fig. 2***C*). We then took advantage of the conserved methionine residue (Met62 in caspase-7 and Met39 in caspase-3) located just N-terminal to the catalytic domain to swap the NTD of caspase-7 with that of caspase-3 (casp3:casp7; **Fig. 2***B*). This transfer failed to restore PARP cleavage, demonstrating that the ability is specific to caspase-7's NTD. Notably, casp3:casp7 is fully active and processes its N-peptide (Supplementary **Table SI** and Supplementary **Fig. 3**). Conversely, we tested the ability of the NTD of caspase-7 to confer PARP cleavage proficiency to caspase-3 (gain of function) by designing a casp7:casp3 chimera (**Fig. 2***D*). In our assay, this chimeric caspase was as efficient as caspase-7 at cleaving PARP. Kinetic analysis demonstrated that casp7:casp3 was 3.6- and 30-fold more efficient than caspase-7 and WT caspase-3, respectively (compare **Fig. 2***E vs*. **Fig. 2***C*). Furthermore, no alteration in the proteolysis of ICAD, a caspase-3-preferred substrate, was observed for this caspase-3 chimera (Supplementary **Fig. 4**).

Because removal of caspase-7's N-peptide precedes its activation (31), we asked if its removal was necessary to the function of the exosite. Thus, we compared a caspase-7 mutant that cannot process its N-peptide due to a D23A mutation (26) and found that this mutant is unable to cleave PARP in our standard assay (**Fig. 2***F*). Importantly, caspase-7_{D23A} does not impair catalytic activity [Supplementary **Table SI** and (26)]. These results demonstrate that the NTD of caspase-7 contains molecular determinants that promote efficient PARP proteolysis.

A basic patch in caspase-7's NTD is critical to promote PARP cleavage. We wanted to identify the critical residues within the NTD that constitute the exosite. To this end, we tested the ability of deletion mutants to cleave PARP. Caspase-7 deletion mutants that lacked NTD residues downstream of Phe36 failed to process PARP in the assay conditions used (**Fig. 3***A*). Conversely, a caspase-7 variant missing residues up to Val32 was still able to cleave the substrate. We also tested tetra-alanine substitution mutants (**Fig. 3***B*) and found that changing residues 37-40 to alanine (mutant 4A4) had a

dramatic effect on PARP proteolysis. These two sets of results suggest that the exosite is present in the basic sequence contained within the NTD. We then fine tuned our assay by lowering the incubation time and caspase concentration to detect the influence of individual residues and scanned the residues contained in the 4A4 mutant (Ser37-Lys40) plus the following Lys41 (**Fig. 3***C*). Unlike the mutation of Ser37, mutation of any lysine hampered, but did not abrogate, PARP cleavage, and K39A and K40A mutations had the greatest effect. The latter result suggests that charge within the exosite is the main determinant. Finally, to further characterize the motif, we designed four mutants with altered charges: K^{38}KKK→AAAA (different from the 4A4 mutant), →KAAK, →KEKK and →KEEK (**Fig. 3***D*). From now on, all K^{38}KKK mutations are referred to using subscript of the four replacing amino acids (WT is caspase-7_{KKKK}). Compared to WT caspase-7, caspase-7_{KAAK} was as efficient at cleaving PARP, whereas a decrease in efficacy was observed as the net charge decreased and negative charges were added. Indeed, caspase-7_{KEKK} was worse than caspase-7_{KAAK}, although both have the same net charge. These results demonstrate that the exosite relies on at least two lysine residues and does not tolerate negative charges. Importantly, all tested mutants displayed proteolytic activity against the peptide substrate that was either similar to the WT enzyme or, if different, could not account for the change in PARP proteolysis (Supplementary **Table SI**).

With the ability to transfer the exosite on caspase-3, these latest results suggest that the exosite is fully contained within the NTD. To further support this conclusion, we performed GST (glutathione-S-transferase) pull-down assays using only caspase-7 residues 24-62. Although GST alone and the tetra-alanine NTD mutant (NTD_{AAAA}) fused to GST failed to bind PARP, the WT NTD readily precipitated PARP (Supplementary **Fig. 5**). Indeed, quantification of the immunoblot signal revealed that 38% of PARP was pulled down. This result was also confirmed by analysis of the post-pull-down supernatant that showed > 50% depletion of PARP. These results show that the NTD contains a complete exosite for PARP.

The NTD of caspase-7 promotes death substrates cleavage in cells. To demonstrate that the exosite supports efficient cleavage of PARP in living cells, we transfected AD-293 cells stably expressing a short hairpin RNA (shRNA; 293^{sh7}) against caspase-7 (Supplementary **Fig. 1***B*) with cDNAs encoding shRNA-resistant flag-tagged caspase-7, caspase-7_{AAAA} or a caspase-7 baring the catalytic mutation C285A. In this paradigm, caspase-7 self-activates and induces cell death without the contribution of any other caspase (26, 32). These constructs also feature the deletion of the N-terminal peptide (M23) to mimic its removal by caspase-3. In agreement with our *in vitro* assays, the K^{38}KKK->AAAA mutation decreases PARP proteolysis (**Fig. 4***A*). Albeit less pronounced than for PARP cleavage, quantification of cleavage products did revealed a decrease of 39% and 26% in the processing of p23 by $M23_{AAAA}$ and Caspase-7_{AAAA}, respectively, compared to the corresponding protein bearing an intact exosite. Importantly, the capacity of caspase-7_{AAAA} to self-activate was assessed by labeling the active enzyme with the activity-based probe biotinyl-VAD-fmk prior to lysis (Supplementary **Fig. 6**). Using this approach, we showed that mutation of the exosite did not impede M23-caspase-7_{AAAA} to self-activate, but did alter full-length processing, which suggests an interaction between the N-terminal peptide and the exosite.

We also used the death ligand Trail to activate the extrinsic pathway in 293^{sh7} cells expressing caspase-7 or caspase-7_{AAAA} at protein levels that do not provoke their autoactivation (**Fig. 4***B*). Using this physiologic death stimulus, cells expressing caspase-7_{AAAA} did processed PARP to a lesser extent compared to cells expressing the WT caspase. Furthermore, time-course of Trail-induced apoptosis showed a 30-60 min delayed in PARP cleavage, but no change in caspase-7 cleavage profile (**Fig. 4***C*). Processing of p23 was also negatively affected by the exosite mutation.

Finally, we used cell-free extracts from 293^{sh7} cells expressing C-terminally flag-tagged WT and caspase-7_{AAAA}, in which we induced caspase activation by the addition of cytochrome *c* (cyt*c*) and dATP leading to the initiator caspase-9 activation. As a source of PARP, we added dialyzed detergent extract from MCF-7^{sh7} cells. Time-course experiments showed a delay in the processing of PARP in extracts reconstituted with caspase-7_{AAAA} (**Fig. 4***D*).

Efficient cleavage of p23 requires the exosite. In **Fig. 1**, we showed that p23 is preferentially cleaved by caspase-7. Consequently, we wanted to extend our finding to p23 by analyzing the ability of key mutants of both executioner caspases to cleave fluorescein-labeled recombinant p23. Importantly, p23 labeling on free amines did not impair p23 cleavage by caspase-7 (Supplementary **Fig. 7**). In an assay in which WT caspase-7 cleaves > 80% of p23, neither M45-caspase-7 nor caspase-3 processed p23 to the cleaved fragments (**Fig. 5***A*). As we have shown for PARP, the casp7:casp3 chimera more efficiently cleave p23. A decrease in p23 cleavage was also observed in cellular experiments expressing caspase-7_{AAAA} (**Fig. 4***A,C*). These latest results demonstrate that caspase-7 also uses the exosite for p23 proteolysis. However, unlike PARP, p23 failed to precipitate with GST-NTD suggesting that the interaction between the NTD and p23 is much weaker.

In order to build a model for the interaction of the caspase-7's exosite with a substrate, we sought to identify regions for which mutations interfere with the cleavage of p23. We used p23 because 1) it is a smaller protein than PARP, 2) cleavage is much slower, which allows us to easily fine tuned the assay, and 3) the exosite is not as dominant as it is the case for PARP, which allows us to better appreciate interference by other region. We built a rational caspase-7 mutant library that incorporated groups of residues that were different in caspase-3 (Supplementary **Fig. 8**). This mutagenesis strategy is very conservative because both executioners share high sequence identity and have identical fold, thus limiting potential adverse effect of mutations. Indeed, all but one (mut8) of the designed mutants are active and self-activate in bacteria (Supplementary **Table SI**). We tested this series of mutants under conditions in which only partial p23 cleavage is obtained. We identified six mutants (mut2, 6, 19, 24, 26, 28) with diminished proteolysis of p23 (**Fig. 5***B*, orange arrows). Mutants 6 (K92DAEA→VDAAN) and 19 (S234PGR→NSKD) are particularly interesting because they are ~0.5 and ~3 times, respectively, more active than WT caspase-7 on the fluorogenic substrate, yet ineffective at processing p23. Remarkably, these two mutants map to the back of the P4 substrate-binding pocket (**Fig. 5***C*). We also identified mutants (mut10, 16, 25, 27) with higher activity toward p23 (**Fig. 5***B*, green arrows). One of them, mut25 (Q276SD→FSF), mapped to the so-called L4 loop, is even less effective at cleaving the peptidic substrate, yet has improved activity on p23. Two more mutants

(mut10, 16) with higher efficiently on p23, localized on the front side of the caspase large subunit enzyme (**Fig. 5***C*). These results suggest that the globular domain of p23 lies close to the catalytic site while binding to the exosite.

Discussion

At minimum, caspases select their substrates based on the structural accessibility of a P1 aspartate motif. To be efficient, however, more determinants are required to restrict the list of candidate proteins. Concretely, initiator caspases must rapidly activate downstream executioner caspases, which then must select among the much larger pool of death substrates to induce cell death. To this end, cells have evolved proficient enzymes, more discriminatory motifs, and presented optimal cleavage sites in flexible loops. In many proteolytic systems, further proficiency is achieved through the usage exosites.

Our results clearly demonstrate that caspase-7 uses a basic patch located in its NTD to improve the proteolysis of PARP and p23, two death substrates. This motif is conserved in mammals, frog and chicken but not in other birds and fish. This domain is whole because it is transferable to another caspase and can precipitate PARP from a cell lysate. The improvement bestowed by the NTD is non-trivial because we observed a ~30-fold decrease in cleavage efficacy when the NTD was removed from caspase-7 and a similar change (~30-fold), but in the opposite direction, upon its transfer onto caspase-3. Furthermore, the fact that lysine mutants and truncated caspase-7 proteins have similar enzymatic properties on the peptidic substrate compared to the WT enzyme argues against an allosteric model involving the NTD. Consequently, we conclude that the tetra-basic motif fulfills all of the requirements of an exosite. This discovery gives credence to a recent study in which it was demonstrated that caspases could not reach proficiency solely by presenting a good cleavage motif (22). Indeed, engineering the best known cleavage motif (DEVD↓G) into a flexible loop in the small subunit of *E. coli* carA protein resulted in a cleavage efficiency by caspase-3 of ~5 x 10^4 $M^{-1}s^{-1}$, which is lower than the cleavage rate observed for PARP with caspase-7, an intrinsically less active enzyme. By comparing the pool of evolutionary unrelated substrates found in the above-mentioned study with the higher cleavage rates of some natural caspase substrates, the authors concluded that caspases likely use exosites to increase catalysis. Another important finding of our study is that the exosite works best if the N-peptide of caspase-7 is removed. During apoptosis, this short 23-amino acid segment is clipped by caspase-3 prior to caspase-7 activation by the initiators, at least in some cells (31), although the involvement of other caspases have not been completely ruled out. We favor a simple model in which the highly acidic N-peptide (9 Asp/Glu residues, no Arg/Lys) shields the basic exosite until it is cleaved.

Caspase-7 mutants with altered activity toward p23, yet presenting opposite or unchanged activity on the peptidic substrate, provide an important structural constraint on the positioning of the substrate to the enzyme. In our model (**Fig. 5***D*), the core of the substrate sits in close proximity to the back of the P4 substrate binding pocket. A second constraint is the requirement for the cleavage site to sit in the substrate-binding pocket. In the case of p23, the length of the C-terminal region spans 49 residues and is

unstructured, (33) which theoretically allows it to reach either catalytic center. However, in the model we proposed, the C-terminal binds the closest active site. This arrangement is analogous to the binding of XIAP to caspase-3 (34), with the second baculovirus inhibitory repeat (BIR2) positioning itself behind the catalytic site and extending its N-terminus over the catalytic cleft, but in a reverse orientation in this particular case. Probably the most interesting feature of our model is that it raises the possibility of a crossed substrate presentation, *i.e.*, the NTD of one catalytic unit provides the exosite for the substrate cleaved by the other catalytic unit within a dimer (**Fig. 5***D*). However, the segment following the basic motif also allows all interactions to take place on the same catalytic unit (direct substrate presentation). It is not certain that the model we have just outlined applies to PARP because this protein has six independently folded domains [reviewed in (35)], thus offering several surfaces for exosite binding. Furthermore, Germain *et al.* demonstrated that caspase-7, but not caspase-3, has affinity for the polyanionic ADP-ribose polymer (PAR) synthetized by PARP as part of its auto-modification activity (17). The protocol we used to extract PARP was not designed to preferentially select modified or unmodified PARP, but may have a bias toward a particular form. We did not use inhibitors of PAR formation and PAR glycohydrolase, and the protocol does not explicitly preserve the energy required for PAR synthesis. Consequently, we favor a model of interaction with PARP itself and not PAR. This is further supported by the ability of the exosite to promote p23 proteolysis, which is not modified, but we cannot rule out an important contribution by PAR to the interaction. Another difference may come from the screening of the caspase-7 mutant library with PARP that did not result in the identification of any determinant other than the NTD, although the strong interaction with the NTD could have masked other determinants. If the proposed model for p23 interaction also holds for PARP, the exosite would bind to the second zinc-finger domain, which precedes the cleavage site.

The interaction of the NTD with p23 is not as strong as it is with PARP. The reason for this is unknown, but it is tempting to speculate that the additional interactions provided by the residues we identified on the catalytic domain of caspase-7 also contribute to p23 cleavage efficiency, thus removing the requirement for strong binding to the NTD. Furthermore, we estimated that p23 is cleaved at least 100 times more slowly than PARP, which cast some doubt on the relevance of its cleavage during apoptosis, at least in the early phase. The simplest answer to explain the large difference in proteolysis rates of PARP and p23 probably resides in the more efficient exosite for PARP (this study) compounded with the favorable aspartate residue at the P4 position of the cleavage site compared to a proline in p23 (7). Other determinants such as secondary and tertiary structures surrounding the cleavage site may also contribute to the difference observed. The p23 promotes ATP hydrolysis and may also specify the client protein repertoire of Hsp90, thus potentially affecting the many activities performed by this system. Furthermore, if many of the roles performed by its yeast ortholog Sba1 are conserved in humans, p23 would play a pivotal role in DNA repair, which is reminiscent of the crucial role of PARP in genome maintenance. Consequently, its proteolysis could have widespread consequences on cellular functions.

Our findings raise the attractive possibility that caspases could use different exosites to achieve their apoptotic and non-apoptotic functions. This multiplicity of

exosites is not unheard of, as some proteases, such as thrombin, use many exosites to bind different substrates and inhibitors. It is likely that other caspases have evolved different exosites to achieve proficiency in their roles during apoptosis and the ever-growing list of non-apoptotic roles of these enzymes.

Materials and Methods

Plasmids. For mammalian cell expression, caspases were expressed with a C-terminal Flag epitope using the pcDNA3 plasmid. The various mutants were generated using standard PCR techniques. A short hairpin RNA construct in pSuper plasmid targeting caspase-7 was created using the following sequences: 5'-gatccccAGACCGGTCCTCGTTTGTAttcaagagaTACAAACGAGGACCGGTCTttttta-3' and 5'-agcttaaaaaAGACCGGTCCTCGTTTGTAtctcttgaaTACAAACGAGGACCGGTCTGGG-3' (capital letters denote the interfering sequence). Caspase-7 resistance to the shRNA was provided by silent mutations of the recognized sequence (underlined nucleotides).

Cell culture and transfection. AD-293 cells were transfected using Lipofectamine 2000 reagent. High-level expression was achieved using 2-4 µg (35/60-mm dishes) of plasmid DNA, whereas lower levels were obtained using 0.25-0.5 µg of the caspase DNA and empty plasmid to 3-4 µg.

Caspase expression, purification and characterization. Recombinant caspase proteins were expressed as C-terminal His_6-tagged proteins in the bacteria and purified using immobilized metal affinity chromatography (IMAC) (26). All enzymes were active site-titrated using the irreversible inhibitor Z-VAD-fmk. The kinetic parameters (k_{cat} and K_M) were determined using the fluorogenic substrate AcDEVD-Afc (36).

Cleavage assays. Cellular extracts containing PARP, ICAD or p23 were prepared from clonal MCF-7 cells stably expressing an anti-caspase-7 shRNA (see above) to reduce potential interference by endogenous executioner caspases. Cells were grown to confluence, washed, and harvested in PBS/EDTA/EGTA. Extracts were prepared in ice-cold buffer [50 mM HEPES (pH 7.4), 150 mM NaCl, 1% NP-40] and incubated on ice for 30 min. The soluble material (detergent extract) was recovered by centrifugation at 7,000 x g for 10 min and kept at -80˚C in small aliquots. A 20- to 30-µl reaction mixture containing detergent extract (1.5-3.5 mg ml^{-1}) was used with 0.5-1.0 nM active-site-titrated protease in caspase buffer at 37˚C for 30-60 min. Assays that used recombinant caspase-9 or p35-C2A were performed similarly by substituting the extracts with purified proteins.

GST (glutathione-S-transferase) pull-down assay. Residues 24-62 from caspase-7 were expressed in *E. coli* as a GST-fusion protein, and purified using glutathione resin. Pull-down assays were performed in caspase buffer containing 2 mM DTT [supplemented with the general protease inhibitors and 10 µM AcDEVD-CHO] using ~10 µg (~3 nmoles) of bound protein, 15 µl of resin and 200 µg of MCF-7^{sh7} detergent extract (1 µg ml^{-1}) overnight at 4˚C. Post-pull-down supernatant and bound proteins were analyzed by immunoblotting.

Hypotonic extracts. Extracts from transfected 293^{sh7} cells were prepared as described elsewhere (3). Caspases activation was programmed by the addition of 1 µM horse cyt*c* and 1 mM dATP to 40 µl of extracts and 20 µl of extracts as a source of PARP. Ectopically expressed caspase-7 levels were adjusted using extracts from empty plasmid-transfected cells.

Recombinant p23 and fluorescein labeling. The p23 cDNA was cloned from a human fetal brain cDNA library, expressed using the pGEX system. Proteins were cleaved with thrombin. The free amines in p23 were trace labeled using NHS-fluorescein in a 2:1 fluorescein:p23 molar ratio. Unreacted labeling reagent and buffer were removed using a 3,000 molecular weight cut-off spin filter.

Acknowledgments

We are grateful to Catherine Duclos and Alexandre Murza for technical assistance and Éric Marsault, Marie-Ève Beaulieu and Pierre Lavigne (Université de Sherbrooke, Canada) for helpful discussion. The PARP plasmid was a gift from Guy Poirier (Université Laval, Canada). This work was supported by grants from the CIHR (MOP-86563) and the NSERC (355388-2010) to J.-B.D.

Authors contribution

D.B. produced and characterized all recombinant caspases, performed cleavage assays and cell-based assays, designed experiments and wrote the manuscript. V.B. generated clonal cell lines. J.-B.D. generated the C7C3 library, performed cellular experiments, designed experiments and wrote the manuscript.

References

1. Galluzzi L*, et al.* (2012) Molecular definitions of cell death subroutines: recommendations of the Nomenclature Committee on Cell Death 2012. *Cell Death Differ* **19**, 107-120.
2. Taylor RC, Cullen SP, & Martin SJ (2008) Apoptosis: controlled demolition at the cellular level. *Nat Rev Mol Cell Biol* **9**, 231-241.
3. Stennicke HR*, et al.* (1998) Pro-caspase-3 is a major physiologic target of caspase-8. *J Biol Chem* **273**, 27084-27090.
4. McStay GP, Salvesen GS, & Green DR (2008) Overlapping cleavage motif selectivity of caspases: implications for analysis of apoptotic pathways. *Cell Death Differ* **15**, 322-331.
5. Pop C*, et al.* (2001) Removal of the pro-domain does not affect the conformation of the procaspase-3 dimer. *Biochemistry* **40**, 14224-14235.
6. Thornberry NA*, et al.* (1997) A combinatorial approach defines specificities of members of the caspase family and granzyme B. Functional relationships established for key mediators of apoptosis. *J Biol Chem* **272**, 17907-17911.
7. Stennicke HR, Renatus M, Meldal M, & Salvesen GS (2000) Internally quenched fluorescent peptide substrates disclose the subsite preferences of human caspases 1, 3, 6, 7 and 8. *Biochem J* **350**, 563-568.
8. Sebbagh M*, et al.* (2001) Caspase-3-mediated cleavage of ROCK I induces MLC phosphorylation and apoptotic membrane blebbing. *Nat Cell Biol* **3**, 346-352.
9. Walsh JG*, et al.* (2008) Executioner caspase-3 and caspase-7 are functionally distinct proteases. *Proc Natl Acad Sci U S A* **105**, 12815-12819.
10. Slee EA, Adrain C, & Martin SJ (2001) Executioner caspase-3, -6, and -7 perform distinct, non-redundant roles during the demolition phase of apoptosis. *J Biol Chem* **276**, 7320-7326.
11. Denault JB, Eckelman BP, Shin H, Pop C, & Salvesen GS (2007) Caspase 3 attenuates XIAP (X-linked inhibitor of apoptosis protein)-mediated inhibition of caspase 9. *Biochem J* **405**, 11-19.
12. Schweigreiter R*, et al.* (2007) Phosphorylation-regulated cleavage of the reticulon protein Nogo-B by caspase-7 at a noncanonical recognition site. *Proteomics* **7**, 4457-4467.
13. Young JE*, et al.* (2007) Proteolytic cleavage of ataxin-7 by caspase-7 modulates cellular toxicity and transcriptional dysregulation. *J Biol Chem* **282**, 30150-30160.
14. Tewari M*, et al.* (1995) Yama/CPP32-beta, a mammalian homolog of CED-3, is a CrmA-inhibitable protease that cleaves the death substrate poly(ADP-ribose) polymerase. *Cell* **81**, 801-809.
15. Los M*, et al.* (2002) Activation and caspase-mediated inhibition of PARP: a molecular switch between fibroblast necrosis and apoptosis in death receptor signaling. *Mol Biol Cell* **13**, 978-988.
16. Oliver FJ*, et al.* (1998) Importance of poly(ADP-ribose) polymerase and its cleavage in apoptosis. Lesson from an uncleavable mutant. *J Biol Chem* **273**, 33533-33539.
17. Germain M*, et al.* (1999) Cleavage of automodified Poly(ADP-ribose) polymerase during apoptosis. Evidence for involvement of caspase-7. *J Biol Chem* **274**, 28379-28384.

18. Malireddi RK, Ippagunta S, Lamkanfi M, & Kanneganti TD (2010) Cutting edge: proteolytic inactivation of poly(ADP-ribose) polymerase 1 by the Nlrp3 and Nlrc4 inflammasomes. *J Immunol* **185**, 3127-3130.
19. Fernandes-Alnemri T, Litwack G, & Alnemri ES (1995) Mch2, a new member of the apoptotic Ced-3/Ice cysteine protease gene family. *Cancer research* **55**, 2737-2742.
20. Van Damme P*, et al.* (2010) The substrate specificity profile of human granzyme A. *Biological chemistry* **391**, 983-997.
21. Quan LT*, et al.* (1996) Proteolytic activation of the cell death protease Yama/CPP32 by granzyme B. *Proc Natl Acad Sci USA* **93**, 1972-1976.
22. Timmer JC*, et al.* (2009) Structural and kinetic determinants of protease substrates. *Nat Struct Mol Biol* **16**, 1101-1108.
23. Fuentes-Prior P & Salvesen GS (2004) The protein structures that shape caspase activity, specificity, activation and inhibition. *Biochem J* **384**, 201-232.
24. Lopez-Otin C & Overall CM (2002) Protease degradomics: a new challenge for proteomics. *Nat Rev Mol Cell Biol* **3**, 509-519.
25. Crawford ED & Wells JA (2011) Caspase substrates and cellular remodeling. *Annu Rev Biochem* **80**, 1055-1087.
26. Denault JB & Salvesen GS (2003) Human Caspase-7 Activity and Regulation by Its N-terminal Peptide. *J Biol Chem* **278**, 34042-34050.
27. Denault JB*, et al.* (2006) Engineered Hybrid Dimers: Tracking the Activation Pathway of Caspase-7. *Mol Cell* **23**, 523-533.
28. Xu G*, et al.* (2001) Covalent inhibition revealed by the crystal structure of the caspase-8/p35 complex. *Nature* **410**, 494-497.
29. Riedl SJ, Renatus M, Snipas SJ, & Salvesen GS (2001) Mechanism based inactivation of caspases by the apoptotic suppressor p35. *Biochemistry* **40**, 13274-13280.
30. Dix MM, Simon GM, & Cravatt BF (2008) Global mapping of the topography and magnitude of proteolytic events in apoptosis. *Cell* **134**, 679-691.
31. Yang X*, et al.* (1998) Granzyme B mimics apical caspases. Description of a unified pathway for trans-activation of executioner caspase-3 and -7. *J Biol Chem* **273**, 34278-34283.
32. Duan H*, et al.* (1996) ICE-LAP3, a novel mammalian homologue of the Caenorhabditis elegans cell death protein Ced-3 is activated during Fas- and tumor necrosis factor-induced apoptosis. *J Biol Chem* **271**, 1621-1625.
33. Weaver AJ, Sullivan WP, Felts SJ, Owen BA, & Toft DO (2000) Crystal structure and activity of human p23, a heat shock protein 90 co-chaperone. *J Biol Chem* **275**, 23045-23052.
34. Riedl SJ*, et al.* (2001) Structural basis for the inhibition of caspase-3 by XIAP. *Cell* **104**, 791-800.
35. Krishnakumar R & Kraus WL (2010) The PARP side of the nucleus: molecular actions, physiological outcomes, and clinical targets. *Mol Cell* **39**, 8-24.
36. Denault JB & Salvesen GS (2007) Apoptotic Caspase Activation and Activity. *Apoptosis and Cancer,* Methods in Molecular Biology, eds Mor G & Rutherford TJ (Humana Press), p 272.
37. Wei Y*, et al.* (2000) The structures of caspases-1, -3, -7 and -8 reveal the basis for substrate and inhibitor selectivity. *Chem Biol* **7**, 423-432.

Figure legends

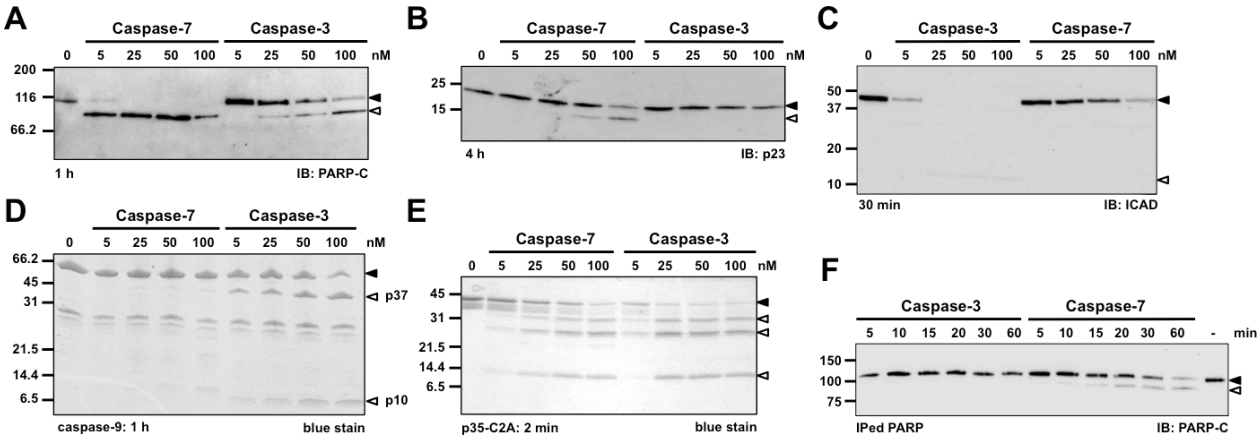

Fig. 1. Caspase-7 is better than caspase-3 at cleaving PARP and p23. (*A*-*C*) MCF-7^{sh7} extracts were incubated for the indicated period of time in the presence of 0, 5, 25, 50 or 100 nM recombinant caspase-7 or -3 in caspase buffer, then samples were analyzed by immunoblotting (IB) using the antibody indicated. (*D,E*) Recombinant full-length caspase-9 (1 µM) or p35-C2A (400 nM) was treated as in (*A*). Samples were TCA-precipitated and analyzed by SDS-PAGE. (F) One nanomolar recombinant caspase-3 or -7 was incubated with immunoprecipitated flag-tagged PARP for the indicated period of time. Samples were analyzed as in (A). Closed arrowhead, full-length protein; open arrowhead, cleaved fragment.

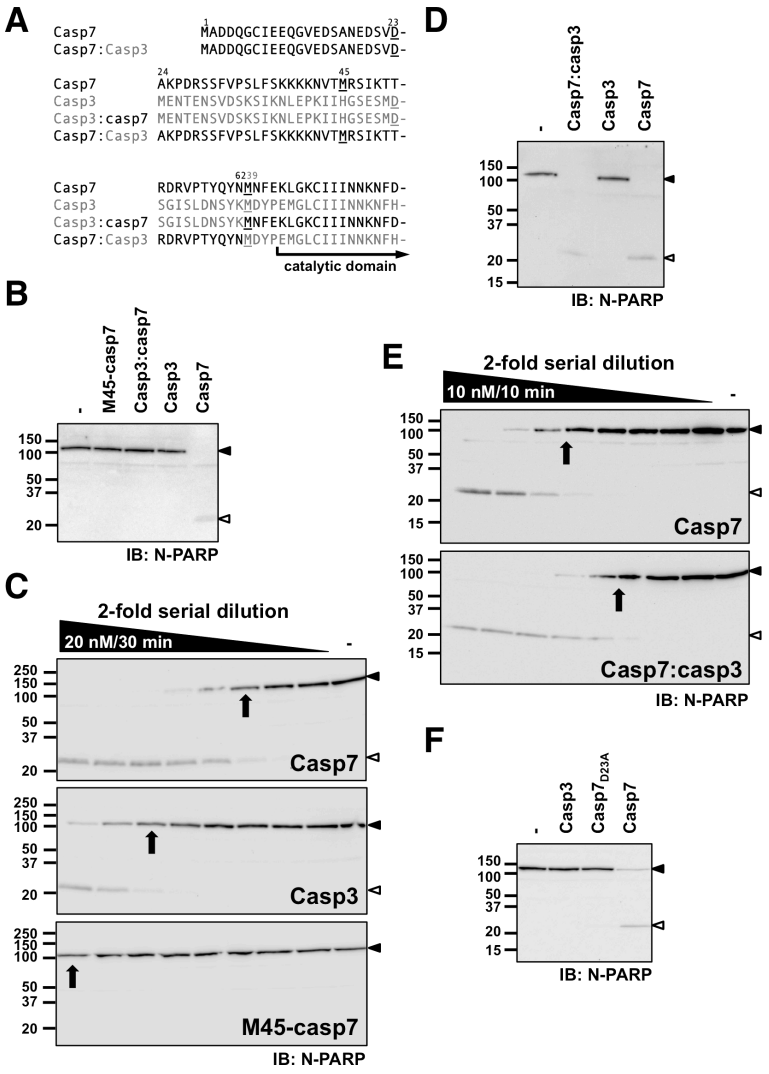

Fig. 2. Caspase-7's N-terminal domain contains a transferable exosite to promote PARP cleavage. (*A*) The amino acid sequence of the N-terminal domain of caspase-7 and -3 are presented. Asp23 of caspase-7 or Asp28 of caspase-3 are the P1 cleavage site residue of the N-peptide that is removed during apoptosis. Mature caspase-7 and -3 start at Ala24 and Ser29, respectively. Key residues are underlined including the conserved methionine used as a convenient location for NTD deletion or chimera design. (*B*,*D*,*F*) MCF-7^{sh7} detergent extracts were incubated for 30 min in the presence of 1 nM of the indicated caspases. Samples were analyzed by immunoblotting using an antibody recognizing the N-terminus of PARP. Quantification of PARP proteolysis is presented in Supplementary **Fig. 2**. (*C*,*E*) Detergent extracts were incubated for the indicated period of time with 2-fold serial dilution of the indicated recombinant enzyme in caspase buffer starting at the indicated concentration. PARP hydrolysis rate were estimated as described in Materials and Methods. The enzyme concentration at which 50% of PARP is cleaved (arrow) was used to estimate rates. In (*C*), the calculated rates are 6.2 x 10^5, <0.2 and 0.8 x 10^5 $M^{-1}s^{-1}$ for caspase-7, M45-caspase-7 and caspase-3, respectively. In (*E*), the calculated rates are 6.5 and 22.1 x 10^5 $M^{-1}s^{-1}$ for caspase-7 and caspase-7:caspase-3 chimera, respectively.

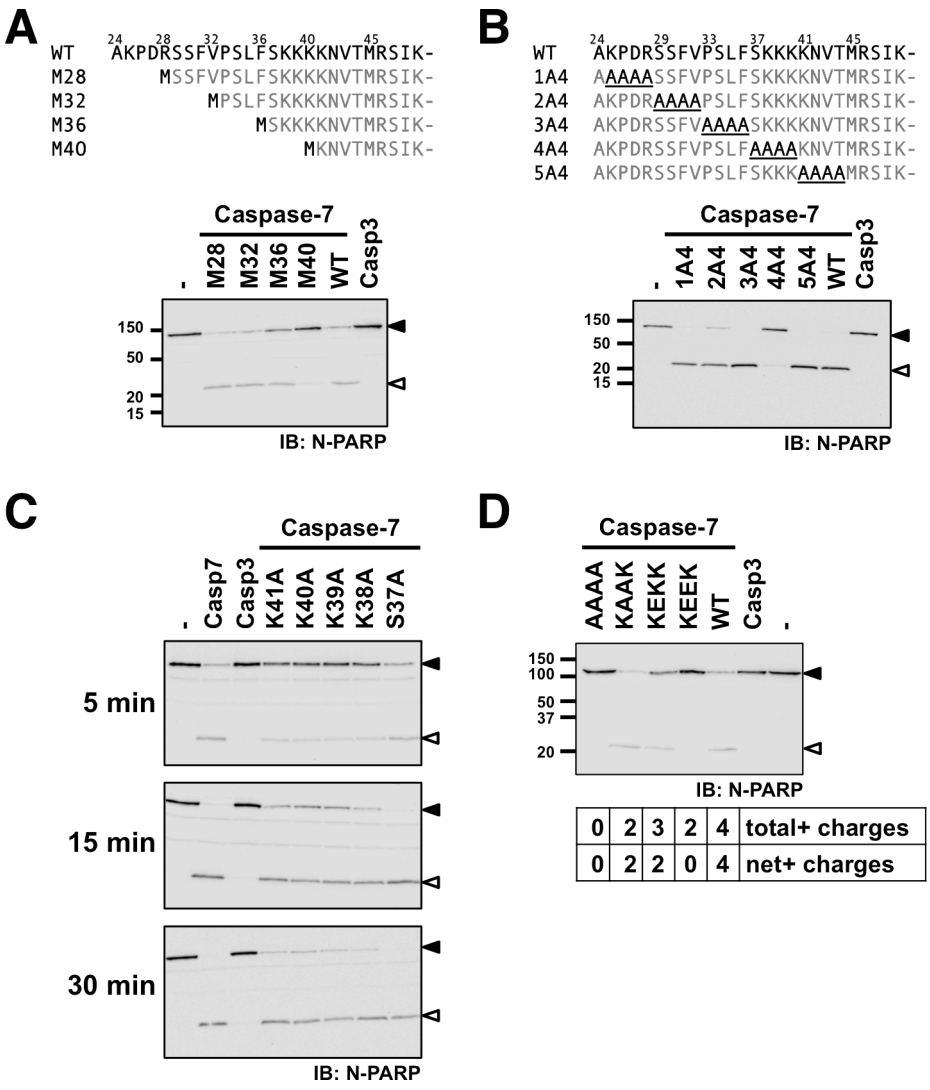

Fig. 3. The $K^{38}KKK$ motif is critical to the exosite function. (*A-D*) MCF-7^{sh7} detergent extracts were incubated for 30 min in the presence of 1 nM of the indicated caspases. Samples were analyzed by immunoblotting using an anti-PARP antibody recognizing the N-terminus. Proteolysis quantification is presented in Supplementary **Fig. 2**.

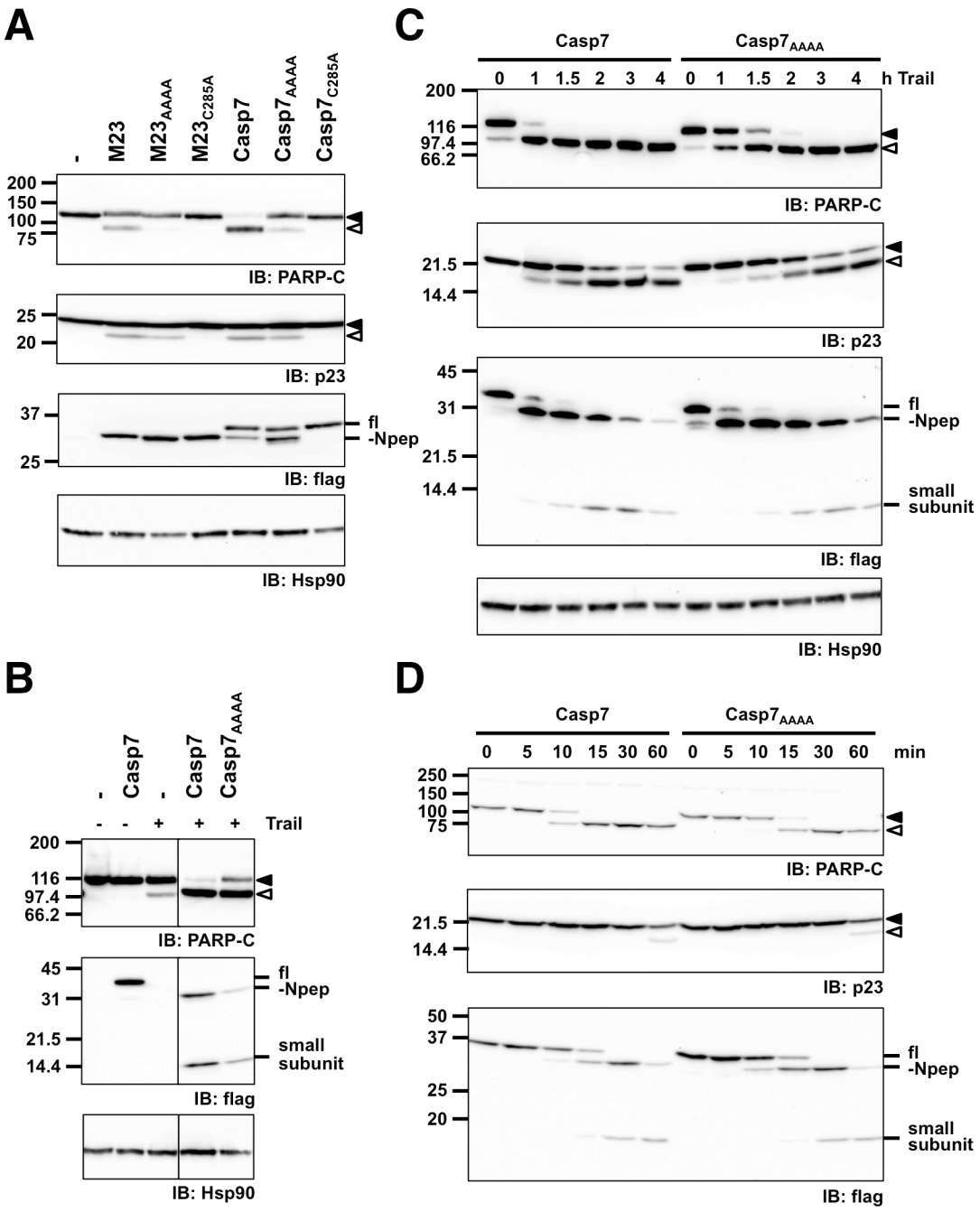

Fig. 4. Efficient PARP proteolysis in apoptotic cells depends on the exosite. (*A*) 293^{sh7} cells were transfected with the indicated flag-tagged shRNA resistant caspase-7 cDNAs. Lysates were analyzed 24 h post-transfection with the indicated antibodies. (*B*) Trail (200 ng/ml)-induced PARP cleavage in cells expressing non-lethal levels of WT or caspase-7$_{AAAA}$. Samples were harvested after 3 h. All lanes were from the same blot. (*C*) Time-course of Trail-induced PARP cleavage in cells expressing non-lethal levels of WT or caspase-7$_{AAAA}$. (*D*) Hypotonic extracts from 293^{sh7} cells reconstituted with low amounts of WT or caspase-7$_{AAAA}$ and supplemented with PARP-containing extracts were activated with cyt*c* and dATP. fl, full-length; -Npep, caspase-7 lacking the N-peptide.

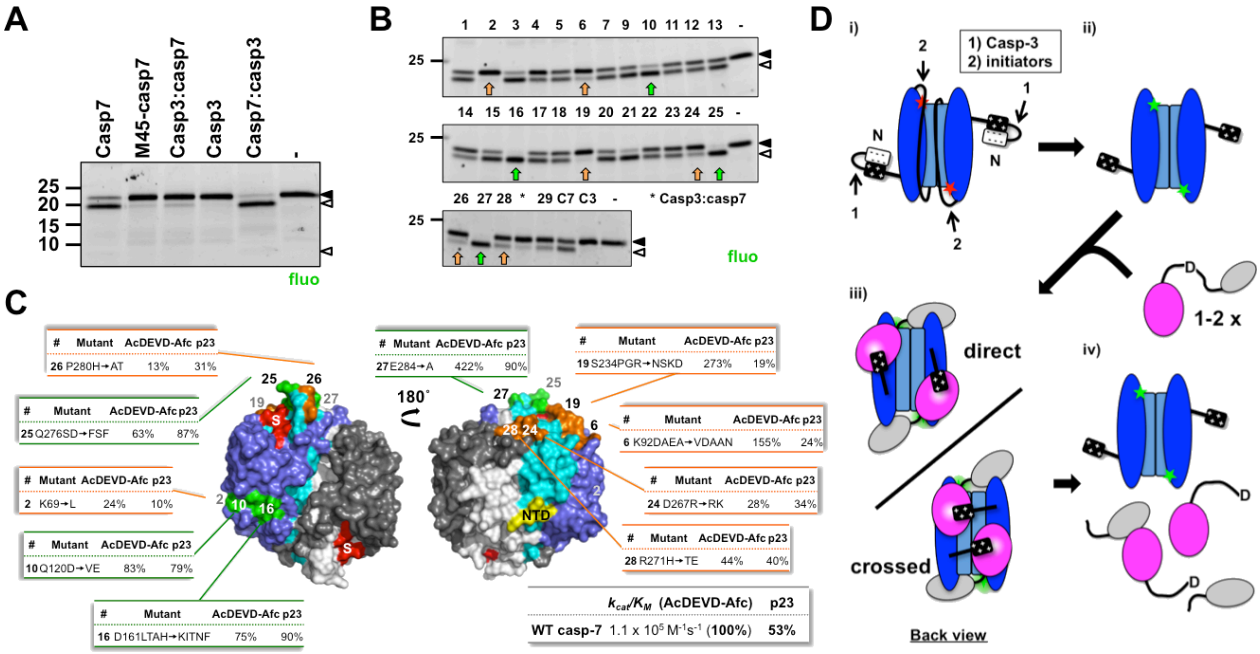

Fig. 5. The exosite promotes cleavage of p23. (*A*) Fluorescein-labeled p23 (50 nM) was incubated with 40 nM of the indicated caspase for 30 min and was analyzed by fluorescence imaging of gels. (*B*) Same as in (*A*) with caspases from the caspase-7:caspase-3 library (Supplementary **Fig. 8**). Mutants showing decrease (orange arrows) or increase (green arrows) in processing are indicated. Mut8 was inactive, therefore not analyzed. (*C*) Surface model of caspase-7 [PDB: 1F1J (37)] presenting the 10 sets of residues identified in (*B*). The dimeric caspase contains two catalytic units, each of them is constituted of a large (blue or gray) and a small (cyan or white) subunits. The active site (S) is identified in red. For each mutant, the relative specific activity (k_{cat}/K_M) *versus* WT for the fluorogenic substrate and the percentage of p23 cleavage are presented. Mut2 lies in a crevasse on the side of the caspase. The NTD is attached at the yellow region. (*D*) Proposed model for the exosite mechanism. *i*) Caspase-3 primes caspase-7 zymogen for activation by removing the negatively charged N-terminal peptide, simultaneously uncovering the basic exosite. *ii*) Then, an initiator caspase activates caspase-7 by cleaving the linker that separates the large and small subunits. *iii*) Up to two molecules of substrates bind the caspase dimer, either in a *direct* or in a *crossed* mode. *iv*) Exosite binding promotes cleavage of the aspartate-containing motif by the catalytic site.

Caspase-7 uses an exosite to promote poly(ADP-ribose) polymerase 1 proteolysis

Dave Boucher, Véronique Blais, and Jean-Bernard Denault

Supporting information

Detailed Materials and Methods

Reagents. Specialized chemicals were obtained from the following sources: G418, isopropyl-β-*D*-thiogalactopyranoside (IPTG) and cell culture media from WISENT Inc. (Montréal QC, Canada); GelCode blue stain and *N*-hydroxy-succinimidyl (NHS)-fluorescein from Thermo Sci. (Rockford IL, USA); glutathione and chelating sepharose 4B fast flow resins from GE Healthcare (Baie d'Urfe QC, Canada); Trail from Enzo Life Sciences (Plymouth Meeting PA, USA); Tropix I-BLOCK from Life Technologies (Carlsbad CA, USA); and thrombin, streptavidin-HRP, dATP, digitonin, horse cytochrome *c* and general protease inhibitors from Sigma-Aldrich (St-Louis MI, USA). Caspase inhibitors and caspase substrates were obtained from BioMol (Farmingdale NY, USA). Other chemicals and molecular biology reagents and enzymes were obtained from general sources.

Plasmids. Human caspase-7 (GenBank acc. no. NM_001227) and human caspase-3 (GenBank acc. no. NM_032991.2) cDNAs were used for all constructs. All recombinant caspase proteins were expressed using the pET-23b(+) (Novagen) plasmid as previously described. (26) For mammalian cell expression, all caspase-7 and caspase-3 proteins were expressed using a modified pcDNA3 plasmid that allowed fusion of the cDNA to a sequence encoding a Flag epitope following an *Xho*I restriction site. Consequently, all expressed proteins contain a C-terminal ELDYKDDDDK sequence and have the native or engineered N-terminus.

Truncation mutants for mammalian expression were generated using standard PCR and an oligonucleotide encoding a Kozak sequence and a 3' reverse primer. All other mutants were generated by overlapping PCR with a pair of oligonucleotides containing the appropriate substitutions and outside primers. Caspase-3/caspase-7 chimeras were obtained by overlapping PCR with oligonucleotides encompassing the chimeric DNA sequence and outside primers. Oligonucleotide sequences are available upon request.

The p23 cDNA was cloned from a human fetal brain cDNA library using a pair of oligonucleotides that inserted a 5' *Bam*HI restriction site and a 3' *Xho*I site. The amplified cDNA was subcloned into the same sites of the pGEX-KG plasmid for bacterial expression.

A short hairpin RNA construct targeting caspase-7 was created using the following sequences: 5'-gatccccAGACCGGTCCTCGTTTGTAttcaagagaTACAAACGAGGACCGGTCTttttta-3'

and 5'-AGCTtaaaaaAGACCGGTCCTCGTTTGTAtctcttgaaTACAAACGAGGACCGGTCTGGG-3' (capital letters denote the interfering sequence). Both primers (20 μM each) were annealed in annealing buffer [30 mM HEPES-KOH (pH 7.4), 100 mM potassium acetate, 2 mM magnesium acetate] and ligated into the *Bgl*II-*Hind*III sites of pSuper. (38) Caspase-7 resistance to RNA interference was provided by the silent mutations of 3 nucleotides within the recognition motif of the mature RNAi (underlined in the above sequence).

Cell culture and transfection. AD-293 (human embryonic kidney cells; Invitrogen caspase, USA) cells were grown in DMEM medium supplemented with 10% v/v FBS, 2 mM L-glutamine and penicillin/streptomycin. Every three days, the cells were either split or provided with fresh medium. MCF-7 cells (human mammary gland adenocarcinoma pleural effusion; ATCC), which do not express caspase-3, were propagated in EMEM medium supplemented as described for 293Ad cells. MCF-7^{sh7} stable cells were established by selecting transfected cells for 14 days using 0.5 mg ml^{-1} G418. Clonal cell lines were obtained from the stable population using cloning rings or 96-well plate seeding (9-11 cells ml^{-1}, 0.1 ml per well). Cells were expanded in the appropriate medium and caspase-7 levels were characterized by immunoblotting.

Cells were transfected with the indicated plasmids using Lipofectamine 2000 reagent (Invitrogen) according to the manufacturer's instructions. High-level expression was achieved using 2 (6-well plates) or 3-4 (6-cm dishes) μg of plasmid DNA. Lower levels of expression were obtained using 0.25-0.5 μg of the caspase plasmid DNA and empty plasmid (3-4 μg final quantities). Cells and debris were harvested at 24 h or the indicated time later in PBS with 1 mM EDTA/EGTA, pelleted by centrifugation, washed in PBS and kept frozen at -80˚C in 10 μl of PBS to facilitate the lysis step. We routinely obtained >80% transfection efficiency based on a β-galactosidase assay.

Caspases were labeled in intact cells with 20 μM biotinyl-VAD-fmk in culture media for 1 h at 37˚C. Then, cells were harvested and kept as described above.

Caspase expression, purification and characterization. Recombinant caspases were expressed as C-terminal His_6-tagged proteins in the BL21(DE3)*pLysS Escherichia coli* strain (Novagen) in 2xYT medium containing 100 μg ml^{-1} ampicillin at 30˚C for 5-20 h to obtain a fully processed active protein. Proteins were purified using immobilized metal affinity chromatography (IMAC) as described elsewhere. With the exception of the caspase-7 5A4 alanine mutant and the casp3:casp7 chimera, for which protein concentrations were estimated based on 80% of the absorbance at 280 nm, all enzymes were active site-titrated using the irreversible inhibitor Z-VAD-fmk as described. The kinetic parameters (k_{cat}, K_M and k_{cat}/K_M) were determined by nonlinear regression using the Michaelis-Menten equation on the velocity data obtained in caspase buffer [10 mM PIPES (pH 7.4), 100 mM NaCl, 10% sucrose, 0.1% CHAPS, 1 mM EDTA and 10 mM dithiothreitol] using a substrate concentration range of 0-300 μM AcDEVD-Afc.

PARP cleavage assays. Cellular extracts containing PARP were prepared from clonal MCF-7 cells stably expressing an anti-caspase-7 shRNA (see above) to reduce potential interference by endogenous executioner caspases. Cells were grown to confluence, washed with PBS (10 mM Na_2HPO_4, 1.76 mM KH_2PO_4, 137 mM NaCl, 2.7 mM KCl), harvested in PBS containing 1 mM EDTA and EGTA and recovered by low speed centrifugation. The following protocol was adapted from published work (39), and is described for a 150-mm plate. We routinely prepared extracts from 8 150-mm plates. The cell pellet was resuspended in 0.2 ml of ice-cold solution 1 [50 mM HEPES (pH 7.4), 150 mM NaCl and 25 µg ml^{-1} digitonin] and incubated on ice for 10 min. After centrifugation at 2,000 x g, the pellet was resuspended by vigorous mixing in 0.2 ml of ice-cold solution 2 [50 mM HEPES (pH 7.4), 150 mM NaCl, 1% NP-40] and incubated on ice for 30 min. The soluble material (detergent extract) was recovered by centrifugation at 7,000 x g for 10 min and kept at -80˚C in small aliquots. The general non-caspase protease inhibitors (1 mM 1,10-*ortho*-phenanthroline, 10 µM E-64, 10 µM leupeptin, 10 µM 3,4-dichloroisocoumarin, 1µM MG-132) were added to all buffers. The PARP cleavage assay was then performed as follows. Unless otherwise mentioned, a 20- to 30-µl reaction mixture containing detergent extract (1.5-3.5 mg ml^{-1}) was used with 0.5-1.0 nM active-site-titrated protease in caspase buffer at 37˚C for 30-60 min.

Assays that used recombinant caspase-9 or p35-C2A were performed similarly by substituting the extracts with purified proteins. Proteins were TCA-precipitated and analyzed by SDS-PAGE. Flag-tagged PARP protein was produced in AD-293^{sh7} cells by transfection. PARP was recovered by immunoprecipitation using the M2 anti-flag antibody, protein A/G beads and eluted using 100 µg/ml^{-1} flag peptide. Proteins were dialyzed to remove excess flag peptide.

PARP hydrolysis rate were estimated using the relation $p = 1\text{-}e^{kEt}$ which correlates the proportion of substrate cleaved to enzyme concentration (*E*), time (*t*) and cleavage rate (*k*). Importantly, the same extracts preparation containing PARP was used for all determinations, which allows relative comparison.

GST (glutathione-S-transferase) pull-down assay. Residues 24-62 from WT caspase-7 were expressed in BL21(DE3) *E. coli* as a GST-fusion protein using the pGEX-KG system. Proteins were purified using glutathione resin in PBS containing 1% Triton X-100. Pull-down assays were performed in caspase buffer containing 2 mM DTT [supplemented with the general protease inhibitors listed above and 10 µM AcDEVD-CHO] using ~10 µg (~3 nmoles) of bound protein, 15 µl of resin and 200 µg of MCF-7^{sh7} detergent extract (1 µg ml^{-1}) overnight at 4˚C. The resin was washed 3 times with caspase buffer, and the proteins were analyzed by immunoblotting. The post-pull-down supernatant was also analyzed to estimate the pull-down efficacy.

Hypotonic extracts. Extracts from transfected AD-293^{sh7} cells were prepared as described elsewhere (3) in a PIPES buffer [20 mM PIPES (pH 7.4), 20 mM KCl, 5 mM EDTA, 2 mM $MgCl_2$ and 2 mM dithiothreitol]. Caspases activation was programmed by the addition of 1 µM horse cytochrome *c* and 1 mM dATP to 40 µl of extracts and 20 µl of dialyzed (8,000 molecular weight cut-off membrane; Spectrum Lab. Inc, Rancho

Dominguez CA, USA) detergent extracts as a source of PARP. Ectopically expressed caspase-7 levels were adjusted using extracts from empty plasmid-transfected cells. Caspase-3 and -7 activity was measured using 200 µM of the chromogenic substrate Ac-DEVD-pNA.

Recombinant p23 and fluorescein labeling. Full-length p23 was expressed in BL21(DE3) *E. coli* as a GST fusion protein using the pGEX-4T-1 system (GE Healthcare). Proteins were purified in PBS containing 1% Triton X-100 using glutathione resin, washed with PBS and cleaved with thrombin (10 U per ml of resin) at 4˚C for 16 h. The free amines in purified p23 were trace labeled using NHS-fluorescein in a 2:1 fluorescein:p23 molar ratio. Unreacted labeling reagent and buffer were removed using a 3,000 molecular weight cut-off Amicon Ultra spin filter (Millipore).

SDS-PAGE and immunoblotting. Cell extracts were prepared by boiling PBS-washed cells for 10 min in 50 mM Tris (pH 7.4), 4 M urea and 1% SDS. Clarified lysates were resolved on continuous SDS polyacrylamide gels using the ammediol buffer system and transferred to polyvinylidene difluoride (PVDF) membrane in 10 mM CAPS (pH 11) and 10% methanol at constant current (0.4 A for 40-60 min). The ensuing blots were processed for immunoblotting with the indicated antibodies and the corresponding HRP-conjugated secondary antibodies (1:7,500; GE Healthcare) and Luminata Crescendo Western HRP substrate (Millipore). The chemiluminescence was monitored using a VersaDoc 4000MP imaging system (BioRad), and the quantification analyses were performed on the non-saturated raw images using the QuantiOne software (BioRad). The following primary antibodies were used: caspase-7 (1:1,1500; 9492; Cell Signaling Technologies), M2 anti-Flag (0.5 µg ml^{-1}; F-3165; Sigma-Aldrich); Hsp90 (0.025 µg ml^{-1}; 610419; BD Transduction Lab.), ICAD (0.17 µg ml^{-1}; PX023A; Cell Sciences); p23 (1:2,000; MA3-414; Thermo Scientific); and PARP [(C-terminus; 1:7,500; 556362; BD Pharmingen) or (N-terminus; 1:7,500; ALX-804-211; Enzo Life Sci.)]. To detect biotinylated proteins, samples were prepared, resolved on SDS-PAGE and transferred onto PVDF membrane as described above, membranes were blocked using 0.2% Tropix I-BLOCK in PBS and revealed using streptavidin-HRP (0.2 µg ml^{-1}) and HRP substrate as above. Broad Range or dual color Precision Plus protein standards were used.

References

1. Denault JB & Salvesen GS (2003) Human Caspase-7 Activity and Regulation by Its N-terminal Peptide. *J Biol Chem* 278, 34042-34050.
2. Brummelkamp TR, Bernards R, & Agami R (2002) A system for stable expression of short interfering RNAs in mammalian cells. *Science* 296, 550-553.
3. Holden P & Horton WA (2009) Crude subcellular fractionation of cultured mammalian cell lines. *BMC Res Notes* 2, 243.
4. Stennicke HR*, et al.* (1998) Pro-caspase-3 is a major physiologic target of caspase-8. *J Biol Chem* 273, 27084-27090.

Supplementary table and figure legends

Table SI Kinetic parameters on AcDEVD-Afc substrate of wild-type and mutant caspases used in this study.

Caspases	K_M (µM)	±	k_{cat} (s^{-1})	±	k_{cat}/K_m ($s^{-1}M^{-1}$)	±
WT and chimeric caspases						
Caspase-7 [1]	31.9	4.6	3.4	0.2	1.1×10^5	0.2×10^5
Caspase-3 [1]	8.8	2.3	5.2	0.4	5.9×10^5	2.0×10^5
Casp3:casp7 [1]	21.8	4.3	7.8	0.5	3.6×10^5	0.9×10^5
Casp7:casp3 [1]	12.5	2.3	9.3	0.5	7.4×10^5	1.7×10^5
Caspase-7 [2] (AcPEVD-Afc)					3.9	
Caspase-3 (AcPEVD-Afc)	95.1	7.7	0.2	0.0	1.9×10^3	1.6×10^2
Deletion mutants						
M23 [3]	68.3	3.8	9.5	0.2	1.4×10^5	n/a
M28	40.8	8.4	14.7	1.2	3.5×10^5	1.1×10^5
M32	32.2	2.2	5.1	0.1	1.6×10^5	1.4×10^4
M36	51.1	3.7	5.6	0.2	1.1×10^5	1.2×10^4
M40	26.2	2.0	6.0	0.2	2.3×10^5	2.5×10^4
M45 [1]	20.6	4.4	2.8	0.2	1.3×10^5	0.4×10^5
Tetra-alanine mutants						
1A4	39.8	3.1	3.5	0.1	8.8×10^4	1.0×10^4
2A4	29.7	3.3	3.5	0.1	1.2×10^5	1.6×10^4
3A4	24.2	2.9	5.6	0.2	2.3×10^5	3.6×10^4
4A4	22.3	1.0	4.7	0.1	2.1×10^5	1.4×10^4
5A4	36.8	1.6	6.65	0.1	1.8×10^5	1.0×10^4
Single alanine mutants						
D23A [3]	68.7	4.5	9.5	0.2	1.4×10^5	n/a
S37A	37.5	2.4	4.4	0.1	1.2×10^5	1.0×10^4
K38A	35.7	1.4	4.3	0.1	1.2×10^5	0.7×10^4
K39A	36.6	1.5	3.9	0.1	1.1×10^5	6.7×10^3
K40A	29.8	1.6	2.9	0.1	9.7×10^4	6.8×10^3
K41A	47.8	2.9	4.1	0.1	8.6×10^4	7.0×10^3
KKKK mutants						
AAAA	31.3	2.0	6.1	0.1	2.0×10^5	5.2×10^4
KAAK	41.1	2.5	8.9	0.2	2.2×10^5	7.7×10^3
KEEK	13.5	0.9	6.2	0.1	4.6×10^5	3.8×10^4
KEKK	25.1	1.1	4.6	0.1	1.8×10^5	1.1×10^4
Library						
Mutant 1	36.6	3.6	1.2	0.1	3.4×10^4	4.7×10^3

Mutant 2	41.8	1.7	1.1	0.0	2.6×10^4	1.4×10^3
Mutant 3	31.6	1.6	2.3	0.0	7.2×10^4	5.0×10^3
Mutant 4	81.8	7.0	4.6	0.2	5.6×10^4	6.8×10^3
Mutant 5	35.9	1.9	4.1	0.1	1.2×10^5	8.4×10^3
Mutant 6	81.2	8.1	13.4	0.1	1.7×10^5	3.0×10^4
Mutant 7	32.0	4.4	1.3	0.1	4.0×10^4	7.4×10^3
Mutant 8	no detectable activity					
Mutant 9	29.5	1.4	2.4	0.1	8.3×10^4	5.3×10^3
Mutant 10	39.8	1.6	3.6	0.1	9.1×10^4	5.1×10^3
Mutant 11	30.2	2.3	3.3	0.1	1.1×10^5	1.1×10^4
Mutant 12	31.7	2.3	3.1	0.1	9.9×10^4	9.5×10^3
Mutant 13	22.4	1.7	2.9	0.1	1.3×10^5	1.0×10^4
Mutant 14	31.1	1.8	2.8	0.1	8.8×10^4	6.8×10^3
Mutant 15	29.3	1.1	3.5	0.1	1.2×10^5	6.0×10^3
Mutant 16	31.7	4.4	2.6	0.1	8.2×10^4	1.5×10^4
Mutant 17	37.7	2.6	0.7	0.0	2.0×10^4	1.8×10^3
Mutant 18	76.4	5.4	1.7	0.1	2.2×10^4	2.2×10^3
Mutant 19	22.8	1.3	6.9	0.1	3.0×10^5	2.3×10^4
Mutant 20	26.8	3.2	1.9	0.1	7.2×10^4	1.1×10^4
Mutant 21	39.6	2.6	2.8	0.1	7.1×10^4	6.2×10^3
Mutant 22	45.8	2.9	3.4	0.1	7.5×10^4	6.4×10^3
Mutant 23	12.2	1.0	2.1	0.0	1.7×10^5	1.7×10^4
Mutant 24	54.7	6.2	1.7	0.1	3.1×10^4	5.0×10^3
Mutant 25	51.6	4.1	3.6	0.1	6.9×10^4	8.2×10^3
Mutant 26	90.9	6.5	1.4	0.1	1.5×10^4	1.6×10^3
Mutant 27	18.2	0.8	8.5	0.1	4.6×10^5	2.6×10^4
Mutant 28	47.5	3.4	2.3	0.1	4.8×10^4	4.8×10^3
Mutant 29	10.6	1.1	3.7	0.1	3.5×10^5	4.6×10^4

[1]: Kinetic parameters were compiled from at least 3 independent determinations and standard errors are reported.
[2]: Kinetic parameters were obtained in pseudo-first order conditions because the K_M is > 100 µM.
[3]: Taken from Denault, J.-B. & Salvesen, G.S. (2003) Human Caspase-7 Activity and Regulation by Its N-terminal Peptide. *J Biol Chem* **278**, 34042-50. n/a, not available.

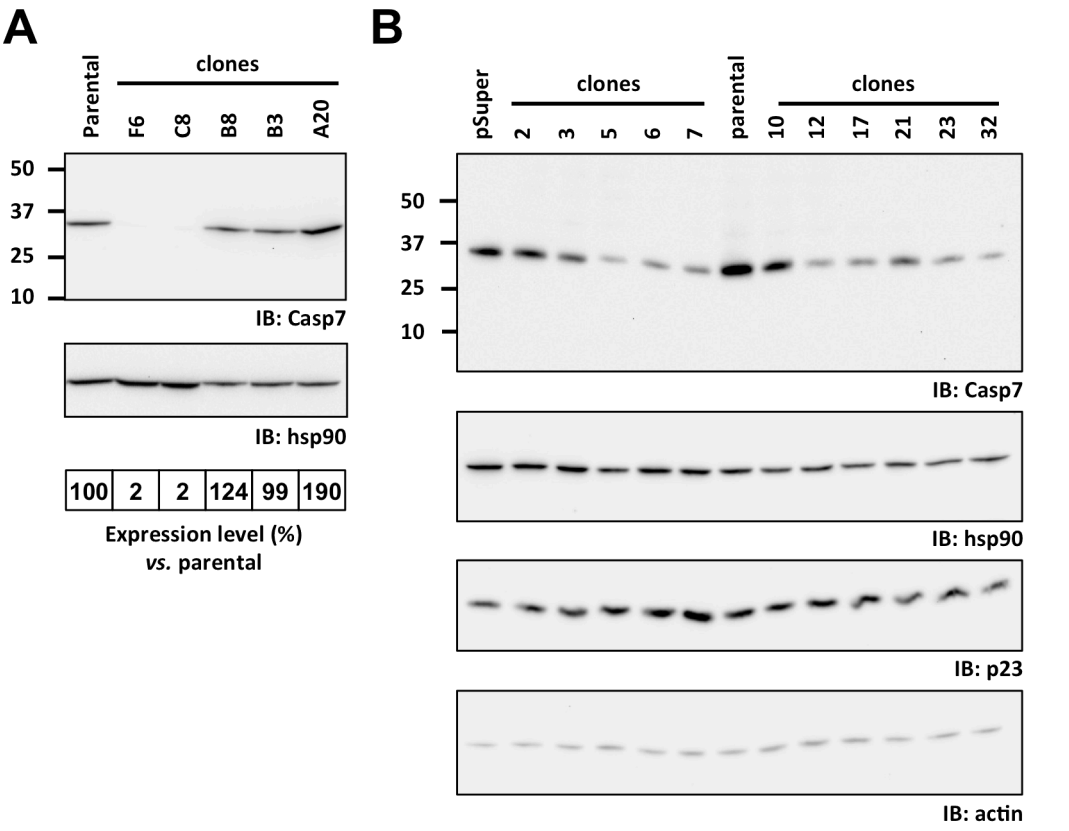

	casp7/hsp90	casp7/actin1	casp7/actin2	casp7/p23
pSuper empty	33%	82%	76%	82%
clone 2	31%	46%	53%	57%
clone 3	17%	24%	27%	33%
clone 5	10%	6%	6%	8%
clone 6	11%	10%	15%	13%
clone 7	14%	11%	14%	10%
Parental cells	100%	100%	100%	100%
clone 10	65%	53%	53%	51%
clone 12	14%	14%	11%	12%
clone 17	22%	16%	13%	14%
clone 21	34%	24%	52%	37%
clone 23	23%	14%	11%	15%
clone 32	**11%**	**11%**	**7%**	**16%**

Fig. S1. Short hairpin RNA-mediated repression of caspase-7 expression in clonal MCF-7 and AD-293 cells. (A) Clonal MCF-7 cell lines were generated using empty pSuper (clones B8 or B3) or pSuper containing a short hairpin RNA against caspase-7 (other clones) as described in Materials and methods. Clones were analyzed by immunoblotting with anti-caspase-7 and anti-hsp90 antibodies. Caspase-7 expression repression was normalized with the control proteins and compared to the parental cells. Clone C8 was chosen to prepare cellular extracts. (B) Clonal AD-293 cell lines were generated using empty pSuper (first lane) or pSuper containing the same short hairpin RNA as in (A). Clones were analyzed as in (A) using a panel of antibodies (2 independent actin quantifications). Clone 32 was chosen.

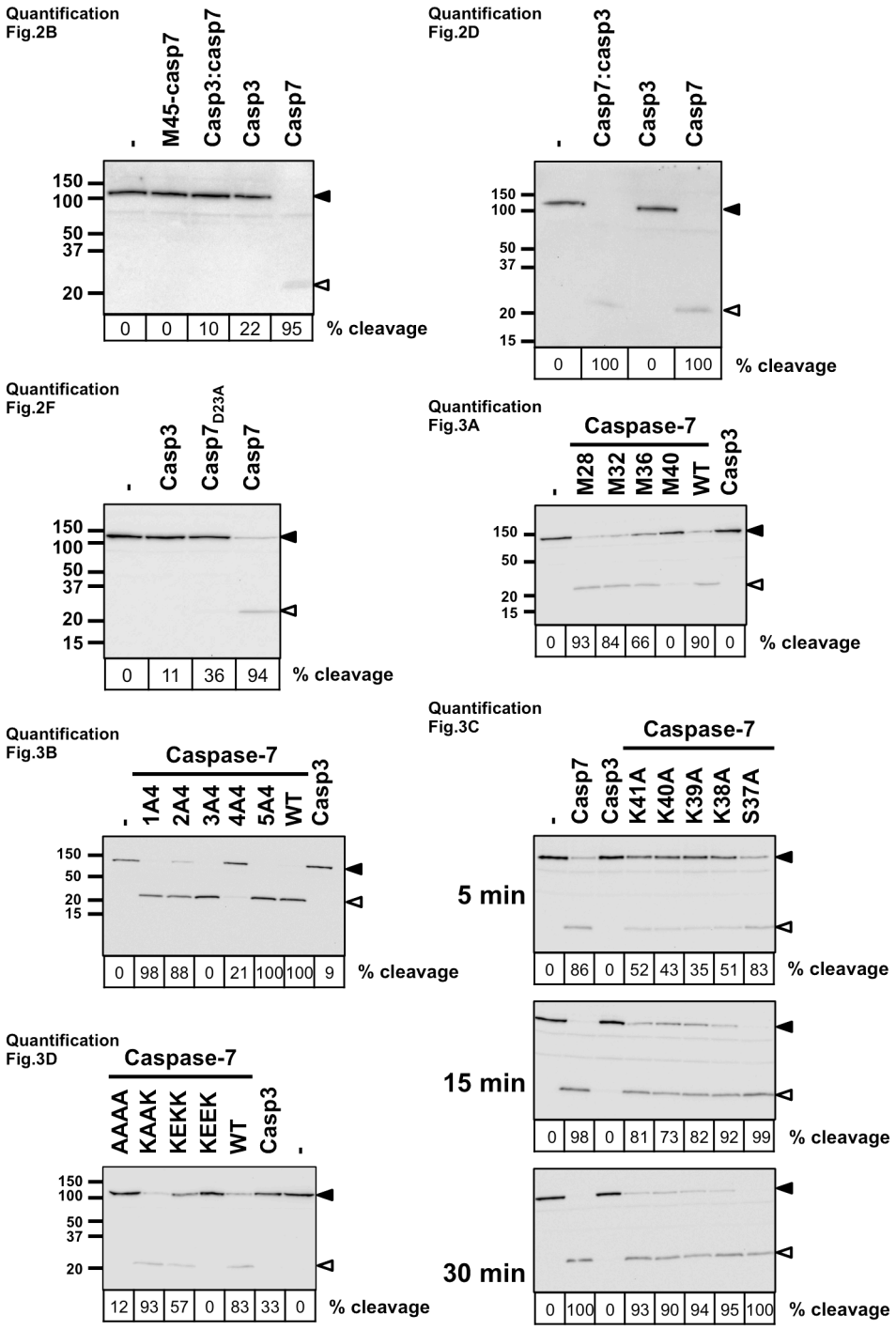

Fig. S2. Quantification of PARP proteolysis from key panels of **Fig. 2** and **Fig. 3**. Results from **Fig. 2***B*,*D*,*F* and **Fig. 3***A*,*B*,*C*,*D* from the main document were further analyzed to determine the percentage of PARP proteolysis. The intensity of the 116-kDa band was quantified using Quantity One software (BioRad) from non saturated exposure acquired on a VersaDoc 4000MP imager. Values are percentages of cleavage compared to the untreated sample figuring on each blots. Blots are labeled as in the manuscript.

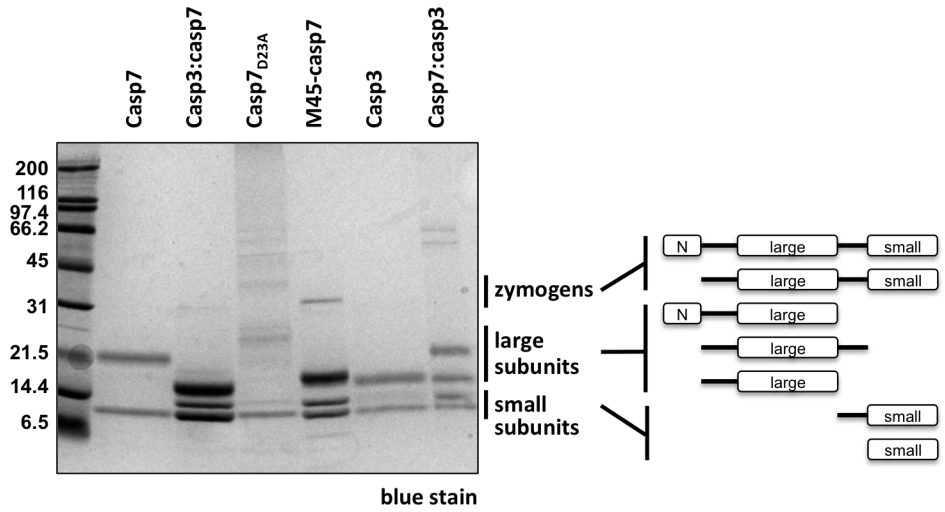

Fig. S3. Bacterial expression and autoactivation of wild-type caspase-3 and -7 and chimeric caspases. The indicated caspase were analyzed on poly-acrylamide gel and visualized using GelCode blue staining reagent. Schematics of proteins obtained after N-peptide removal and cleavage at activation sites are presented on the right.

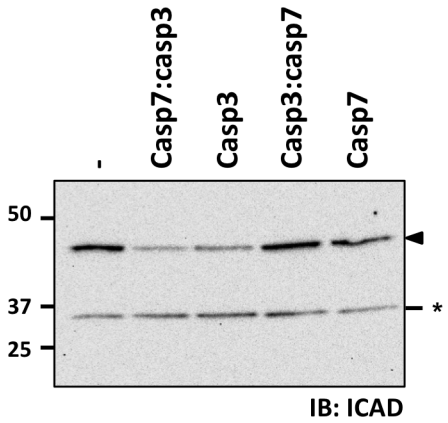

Fig. S4. Caspase-3 or -7's NTD does not confer preference for ICAD cleavage. Detergent extracts were incubated for 15 min in the presence of 10 nM of the indicated caspase in caspase buffer, and then analyzed by immunoblotting using an anti-ICAD antibody. The asterisk indicates a non-specific band recognized by the antibody and serves as a loading control. Closed arrowhead, full-length protein.

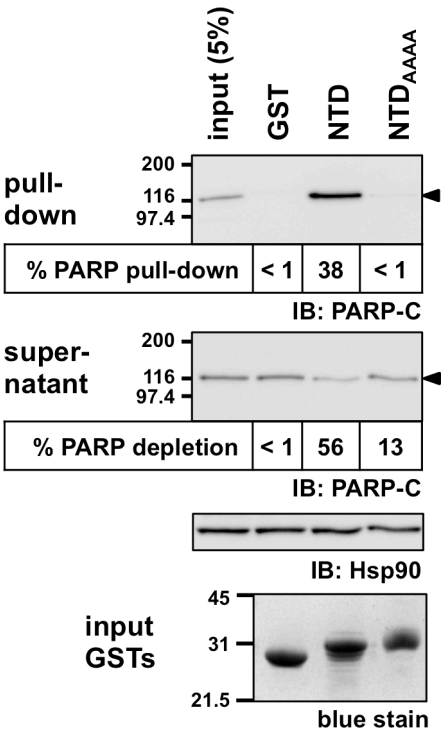

Fig. S5. Caspase 7's NTD binds PARP. Ten µg of GST, GST-NTD or GST-NTD_{AAAA} on beads were incubated with 200 µg (1 mg ml^{-1}) of MCF-7sh7 extract for 16 h at 4˚C. Pull-down proteins (*top*) and equal proportion of post pull-down supernatant (*middle*) were analyzed by immunoblotting with the indicated antibodies. Blots were quantified to determine pull-down and depletion efficacy and are presented as percentage of total PARP protein used in each samples. SDS-PAGE analysis of GST proteins is presented (*bottom*).

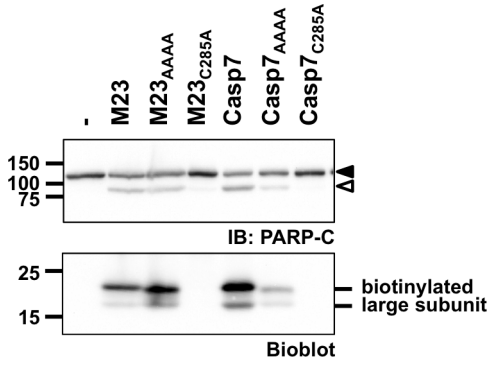

Fig. S6. Labeling of caspase-7 and caspase-7_{AAAA} in intact cells. Twenty-four hours post-transfection, cells as in **Fig. 4***A* were incubated for 1 h with 20 μM of the cell permeable biotinyl-VAD-fmk irreversible caspase inhibitor. Extracts were prepared and analyzed by immunoblot using an anti-PARP antibody or using streptavidin-HRP to revealed biotinylated (active) caspase-7 (bioblot). Closed arrowhead, full-length protein; open arrowhead, cleaved fragment.

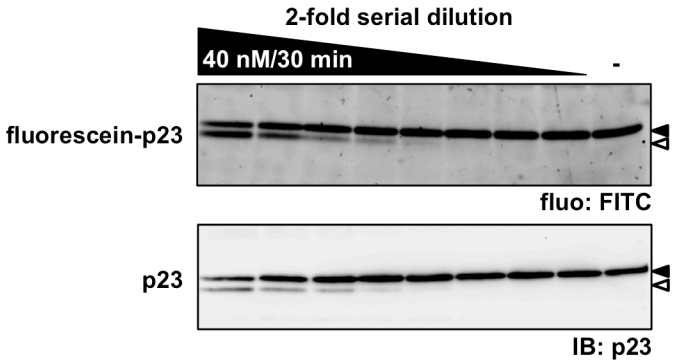

Fig. S7. FITC-labeled and unlabeled p23 are cleaved as efficiently by caspase-7. Unlabeled or fluorescein labeled purified recombinant p23 (50 nM) was incubated for 30 min with 2-fold serial dilution of recombinant caspase-7 in caspase buffer starting at a caspase concentration of 40 nM. Samples were analyzed by fluorescence imaging (*top*) or immunoblotting (*bottom*) using an anti-p23 antibody. It is noted that no more than a 2-fold difference in cleavage efficiency was observed. Closed arrowhead, full-length protein; open arrowheads, cleaved fragments.

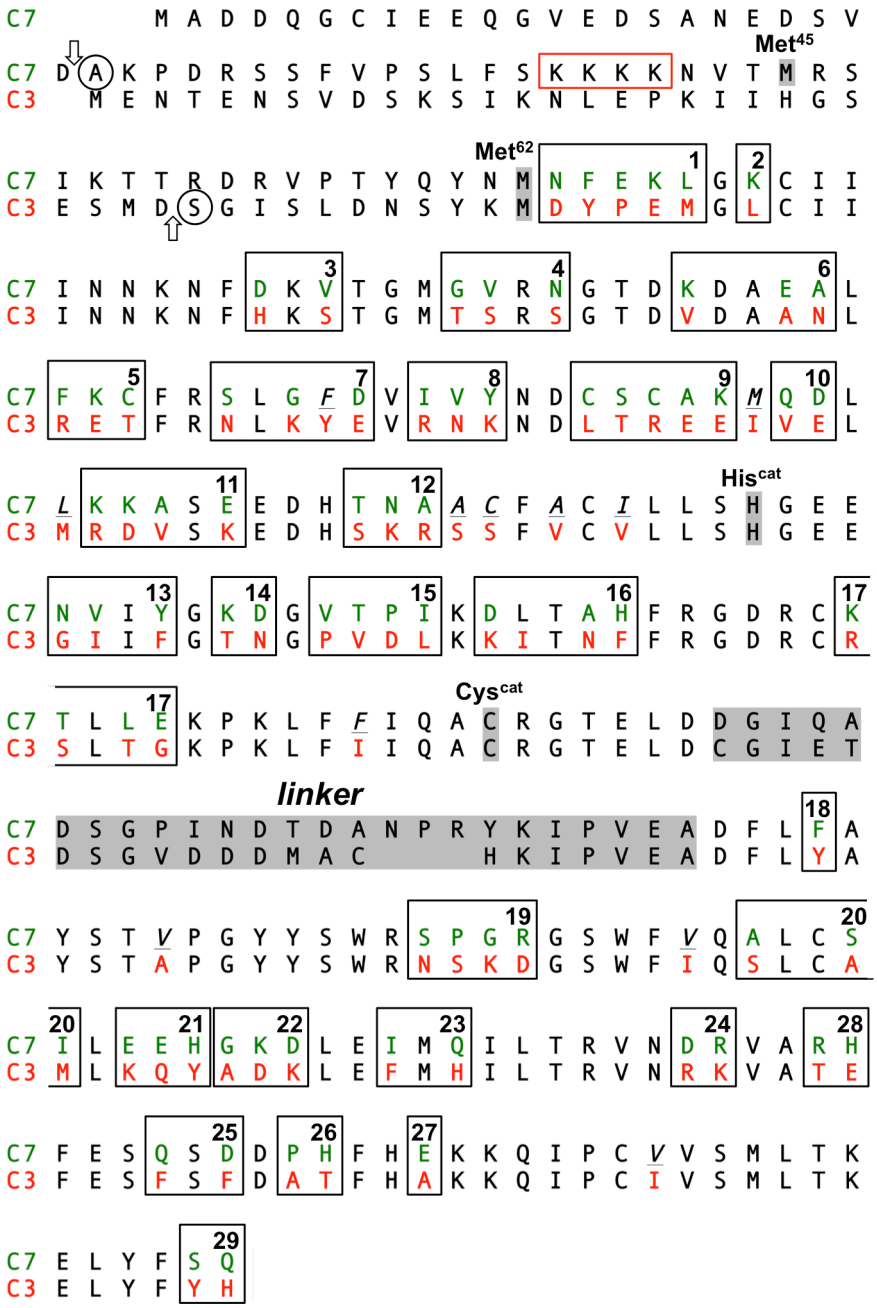

Fig. S8. Rational design of the caspase-7:caspase-3 mutant library. Alignment of caspase-7 and caspase-3 primary sequence. Boxed residues correspond to mutants in which amino acids from caspase-3 were substituted in caspase-7. Italicized and underlined residues were not mutated because they are buried into the structure. The catalytic cysteine and histidine along with the methionine 62, which was used to create chimeric caspases, and methionine 45 are indicated. The N-terminal residue of the mature form of each caspases resulting from the removal of the N-peptide is circled. A red box indicates the tetrabasic patch. The linker that separates the large and small subunit is shadowed and was left unchanged.